
Article:
Gomez, Leonardo Dario orcid.org/0000-0001-6382-9447, Lanigan, Joseph L., Faas, Laura et al. (4 more authors) (2024) Pressure induced transformation of biomass to a highly durable, low friction film on steel. Proceedings of the Royal Society A: Mathematical, Physical and Engineering Sciences. 20230450. ISSN 1364-5021

https://doi.org/10.1098/rspa.2023.0450

PROCEEDINGS A

royalsocietypublishing.org/journal/rspa

Research

Cite this article: Lanigan JL, Faas L, Butcher T, Skipper WA, Silva MP, Lewis R, Gomez LD. 2024 Pressure induced transformation of biomass to a highly durable, low friction film on steel. *Proc. R. Soc. A* **480**: 20230450. https://doi.org/10.1098/rspa.2023.0450

Received: 20 June 2023
Accepted: 9 January 2024

Subject Areas:
mechanical engineering, biochemistry, analytical chemistry

Keywords:
tribology, wheel/rail interface, thin films, surface analysis

Author for correspondence:
Joseph L. Lanigan
e-mail: j.lanigan@sheffield.ac.uk

†Denotes the main authors, these authors contributed equally to this work.

Electronic supplementary material is available online at https://doi.org/10.6084/m9.figshare.c.7055530.

THE ROYAL SOCIETY PUBLISHING

Pressure induced transformation of biomass to a highly durable, low friction film on steel

Joseph L. Lanigan[1,†], Laura Faas[2,†], Thomas Butcher[1], William A. Skipper[1], Mariana P. Silva[2], Roger Lewis[1] and Leonardo D. Gomez[2]

[1]Department of Mechanical Engineering, The University of Sheffield, Mappin Street, Sheffield S1 3JD, UK
[2]Centre for Novel Agricultural Product, Department of Biology, University of York, Wentworth Way, York YO10 5DD, UK

JLL, 0000-0001-9860-9559; TB, 0000-0002-7996-1132; RL, 0000-0002-4300-0540

Herein the authors report a detailed insight into the tribological and chemical mechanisms that take place when leaf matter is present at the wheel/rail interface. The approach used enables further insight into the formation and subsequent effects on friction from leaf derived layers. Results shed insight on the process that facilitates the formation of leaf derived layers, their structure and chemical make-up. Our analysis indicates that polyphenols, a chemical family that include tannins, have an important role in layer formation and hypothesis on the layer's stability, when formed under high pressures. The data indicate that the high pressure found at the wheel/rail interface facilitates conversion of biomass into a tenacious, thin film. This is shown by the increase in the amount of phenolic compounds present. Phenolic compounds are typically rich in oxygen functional groups that have the ability to bind to metal ions. This insight into the composition of the film is expected to enable the development of novel remediation strategies. It highlights the potential for cleaning

agents to be used as tools for restoring friction to safe values. This should lead to improvements in the operational performance and safety of rail transport for passengers and train operators.

1. Introduction

(a) Leaves on the line

'Leaves on the line' is a well-known challenge across railways around the globe that involves the formation of a low friction, leaf derived 'black layer' on the rail head. These leaf layers can have a negative impact on the braking performance of passenger and freight vehicles, resulting in compromised operational performance and in extreme cases safety issues. This is because the layer is known to be difficult to brake upon, due to its low friction properties. It also presents difficulties for acceleration, which in turn can result in train delays. These issues incur significant costs to the industry and end-users in terms of delayed-travel time and the necessity of using treatments to restore the railhead to an uncontaminated state [1].

Considerable research has been conducted into the frictional properties of the leaf layers that form on the railhead (anecdotally known by rail workers as 'black layer', due to the film's typical coloration). The evidence available at present establishes that the 'black layer' is indeed a cause of low friction (defined as being below 0.05 [2]) on the railway. Further work on the mechanism of formation and lubricity of the layer has been ongoing to understand what this tenacious, low friction, thin film is formed of. This will enable better remediation strategies and improved operational performance. However, there is a lack of detailed knowledge of the composition of the 'black layer' and how leaves are converted, after falling on or near the line, into this thin film.

Previous research has underlined the role of weather conditions and train frequency in this process [3]. The present work explores the mechanism behind the transformation of leaf material on the railhead. Factors affecting this transformation include the high pressures at the contact, often reported as 800 MPa, although there is a broad range surpassing 1 GPa [4,5], as well as the high temperature (within the wheel/rail contact patch, or 'running-band') and the presence of catalytic metals present at the wheel/rail interface. The typical reaction product of cellulose (a major component of biomass) under pressure and heat is 'char', a pyrolysis product [6].

Hyperbaric (400 MPa) treatment of cellulose (without the presence of steel, or iron) has been studied by nuclear magnetic resonance (NMR) studies of carbon^{13} and infrared spectroscopy [7]. Under these conditions, only minimal changes to cellulose, described as 'increased crystallinity', were observed.

In this work, an increase in polyphenol content coupled with a decrease in cellulose and hemicellulose is observed. Pectin content appears largely unchanged. This is highly indicative of a different reaction pathway, likely facilitated by the presence of a known catalytic species (iron oxide) at a high-enough heat and pressure. Other iron salts (such as iron nitrate) exhibit catalytic activity toward biomass and specifically cellulose [8,9]. Interestingly, the authors did not note graphitization as has been seen when iron nitrate is present. This suggests the reaction pathway is highly sensitive to: pressure, heat and the metal present [7].

Previous research has attempted to establish the roles of pressure, temperature and catalytic metal(s), although mechanistic insight regarding the key low adhesion species present at the interface is lacking, specifically with samples obtained from field testing [5,10–15].

(b) Current and future solutions

Remediation measures are employed by Network Rail and other rail infrastructure managers for cleaning the railhead in the UK. These include very high-pressure water jetting using railhead treatment trains (RHTTs) for the susceptible routes. There are also chemical approaches for more

localized remediation of the black layer. Other approaches are used to increase traction in the wheel/rail interface such as sand application from systems on-board trains or use of traction gels which are laid directly onto the railhead.

The cleaning agents usually include an organic solvent with a surfactant. Among them, there is a family of products that contain a solvent derived from citrus fruit peel. Various brands exist with modifications on the name 'citra-sol', 'citra-solv' and 'citrus-cleaner', etc. all of which contain D-limonene [16]. D-limonene is an organic solvent, however, it has not been tailored for use within the rail industry. These cleaning products are not designed for the specific purpose of removing biomaterials like those found in railhead films. D-limonene was initially proposed as an industrial replacement for chlorinated-hydrocarbons solvents [17]. In laboratory conditions, extended heating is required for optimal solvent efficiency of biological components [18]. Additionally, their use typically necessitates additional manual labour on the railway, which adds considerable risk; even with all required safety measures in place.

There are marked drawbacks with each of the techniques mentioned, from availability of treatment trains (RHTTs) to effective access to remote areas of high vegetation, as well as safe disposal of resultant chemical waste. The solutions employed should be compliant in the UK with the commitment to maintain the railway as a 'biodiversity corridor', as they are one of the few very long stretches of relatively undisturbed countryside that acts as home to many rare species of plants and animals [19].

Novel techniques for cleaning the railhead are being developed and are showing promise in terms of mobility benefits. That is to say, some newer methods of rail cleaning can either be mounted on road-to-rail vehicles or passenger trains and thus are capable of accessing more remote areas or locations that may not have frequent RHTT treatments. In addition, some of these methods could reduce energy use compared to the RHTT. These include methods that employ dry ice as the cleaning agent, which sublimes leaving no chemical residue after cleaning [20,21].

(c) Current understanding of the leaf layer

Several surface sensitive techniques have been applied to leaf films in the laboratory, as well as in the field, in an effort to understand the composition of the layer.

A combination of spectral data, including X-ray photoelectron spectroscopy (XPS) and Fourier-transformed infrared spectroscopy (FT-IR), have confirmed the presence of 'organic' (that is to say, predominantly carbon–carbon bond containing) species. Organic species are composed of predominantly carbon, oxygen and hydrogen; although hydrogen is undetectable via techniques including XPS.

Additional trace elements (typically of mineral origin) vary across sample locations, but usually include elements associated with steel alloys, residual traces of remediation techniques or other rail infrastructure items. These are prominently various forms of silicon and iron [22,23].

Silicon, or more specifically silica/sand, is routinely employed during braking from systems on-board trains and is also a known component of traction gels. Traction gels are products designed to raise friction at problem hotspots [24]. Combined spectral analysis has developed our understanding of the chemical bonds present in the film. FT-IR typically indicates these films contain C–H and –OH bonds as well as the presence of C=O, or carboxyl groups [15].

Although these spectral studies are very useful, they should be complemented by biochemical analyses to enhance understanding of the composition of the layer. Recent advances by Watson *et al*. [23] suggested that tannins (a component of leaves and a type of polyphenols) could play an important role in the observed low friction. FT-IR data have since added evidence indicating the presence of iron chelate compounds.

Chelate compounds in this instance refer to metal ions being bound to an organic molecule, usually through formation of semi-stable, metal–oxygen bonds. In this instance iron (Fe) interacts with oxygen containing compounds in the film (L.F. and L.D.G. 2023, unpublished data). Chelates are well known in various applications, an example of their use in the household is with kitchen/bathroom sprays designed to remove lime scale, or calcium carbonate. Here, the energy

associated with chelate formation is able to displace the carbonate salt and form a chelated calcium compound that is easily washed away.

Interestingly, iron tannates have been used in ink as iron gallate in the past, demonstrating its ability to form films on paper rapidly [25]. Iron gallate is the product of the reaction between tannic acid, a polyphenol and iron. The reactivity of iron on the railhead is well known, prominently by its tendency to oxidize over time when exposed to air and water. Many 'Lewis acids' are able to catalyse reactions. A 'Lewis acid' differs from more common acids like hydrochloric acid (or other species where a proton, H^+ acts as the acid). Instead, a metal is able to function in the same way, by accepting an electron pair from OH^- (hydroxide) species [26].

A number of these are used commercially with Fe as the metal ion due to its capacity to react with a variety of materials including biomass [9,27].

An additional indicator regarding the film's role in reducing the friction on the rail is its resistance to wear coupled with its low friction properties. These properties are shared with compounds like tannins or polyphenols, both of which have 6-member carbon rings with π-electrons. These are known to exhibit great chemical stability, known as aromatic stabilization [28–30]. The chemical composition of fallen leaves includes both soluble and insoluble phenolic compounds, such as tannic acid, gallic acid and free phenolic acids [31]. This can be linked to established tribological mechanisms of low traction as molecules like phenolic compounds share the feature of having a large portion of delocalized electrons (or π-bonds, as seen in phenol and benzene) and exhibit planar characteristics (in terms of their molecular shape).

Phenolics, including tannins, are relatively abundant in leaves and may be transformed to more complex polyphenols under the appropriate conditions. The chemical conjugation of phenolics requires heating and mechanical mixing in the presence of a solid catalysis like iron trichloride or alumina [27,32]. In the present work, we performed a biochemical analysis on leaf layers produced under typical wheel/rail contact conditions in the laboratory and in the field using an actual locomotive. The aim of this was to further the understanding of the composition of the layer produced, as well as the process driving the transformation of leaves into films [21].

2. Material and methods

Several experimental methodologies were employed during the course of the research; these will be explained in detail below. The methodologies required sourcing of some chemical reagents as well as other raw materials. Chemicals were obtained from the suppliers listed below. Leaf samples from different tree species were collected during the UK leaf fall season.

(a) Raw materials

(i) Leaves and organic matter

Leaves were sourced in Yorkshire, dried at 70°C and preserved for testing after being ground to 1 mm particle size using an impact mill (Restch).

In addition, oak bark powder was sourced for use in some tests. This decision was made as, despite tree bark's dissimilarity with leaves, it can be purchased as a standard for repeatable testing. Oak bark was sourced commercially and purchased from 'Alfa Aesar'.

(ii) Graphite

The solid lubricant, graphite, was sourced from 'Alfa Aesar'. It was obtained as a synthetic graphite powder with an average particle size of 7–11 µm at 99% purity (CAS no.: 7782-42-5). Graphite was purchased for testing as its effects on friction and mechanism by which it exerts these are well understood and detailed in the literature. This dataset enables greater insight into the mechanisms of friction of other components.

Figure 1. Formation of the leaf layer at QRTC.

(b) Methodologies

Leaf layers were created and tested in a laboratory setting as well as in the field. The techniques used for each are detailed below.

(i) Creation of leaf layers in the field

A representative thin film was created at a private railway in the UK (figure 1). The methodology for formation of the layer was adapted from previous work undertaken at the site, QRTC (Quinton Rail Technology Centre, Stratford-upon-Avon, UK) [22]. The methodology has been adapted to reduce total layer formation time. Initially, leaf powder was evenly spread on to a clean, pre-wetted (with deionized water) railhead. A diesel shunter then passed over the film without braking a minimum of five times for each leaf material tested. After this, a braking pass was undertaken, adding the shear force needed to accelerate the formation of the 'black layer' observed on track.

Samples were taken before testing, after the rolling passes and finally after the braking pass. These samples were then subjected to in-depth biochemical analysis.

(ii) Testing of leaf layers using a high-pressure torsion approach

Laboratory-controlled testing was achieved using the high-pressure torsion (HPT) test rig, previously used for rail applications [33,34]. A schematic of this is shown in figure 2. This test method was used over twin-disc type tribometers as it ensures the materials tested remain in contact for the duration of the testing. Thus the materials at the interface experience the high pressures and temperatures associated with the wheel/rail interface.

Testing on the HPT rig comprises a bottom specimen (R260 rail steel) with a top specimen (R8T wheel steel). Both samples were created from sections of a rail wheel and rail steel parts. The heat treatment used by the manufacturer to create R8T steel has not been disclosed to the authors. Information on the alloys available in the literature is given below (table 1).

The samples are compressed together and create an annular contact, which allows third bodies to be applied uniformly. Torque can be applied to the bottom specimen moving it through a set sweep length and speed (less than 1 mm s^{-1}). The HPT rig is shown in figure 2, where (1) and (2)

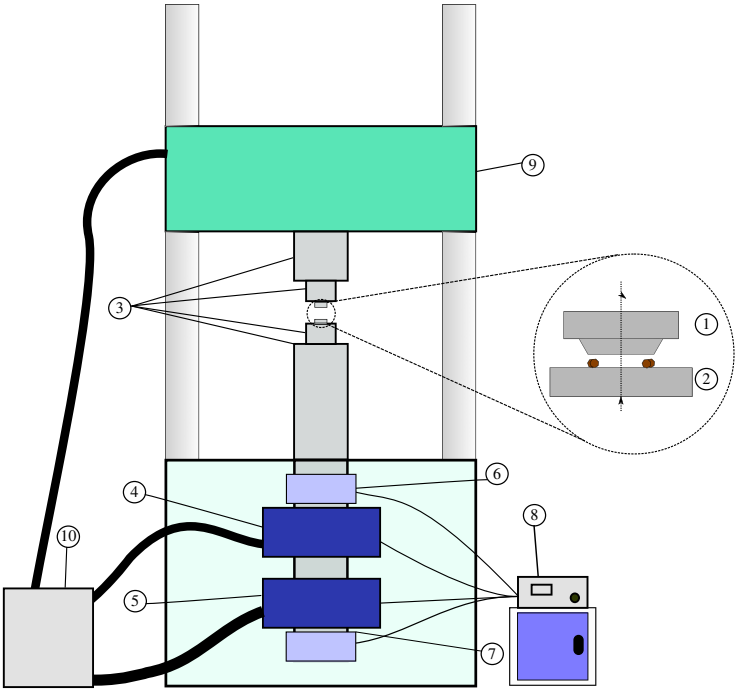

Figure 2. Schematic of the HPT test rig [35].

Table 1. Reported literature values for chemical composition and hardness values of rail alloys tested (where 'n.d.' represents non-detected).

element %wt	R8T	R260
Al	n.d	≤0.004
C	0.56	0.62
Si	0.4	0.15
Mn	0.8	0.7
Mo	0.08	n.d.
Cr	0.3	≤0.15
Ni	0.3	n.d
S	0.015	0.008
P	0.02	≤0.025
V	0.06	≤0.03
hardness (HV)	260	287

denote the top and bottom specimens, respectively; any desired third body layers were applied to the surface of the bottom specimen; specimens were held in place by manufactured sample holders (3). Axial position/force was controlled via a linear hydraulic actuator (5) and axial feedback was measured by a linear variable differential transducer (LVDT)/load cell (7). Torsional position/force was controlled via a rotational hydraulic actuator (4) and torsional feedback was measured by a rotary variable differential transducer (RVDT)/load cell (6). The controller (8) regulated the hydraulic actuators and recorded feedback from the LVDT/RVDT/load cells. The

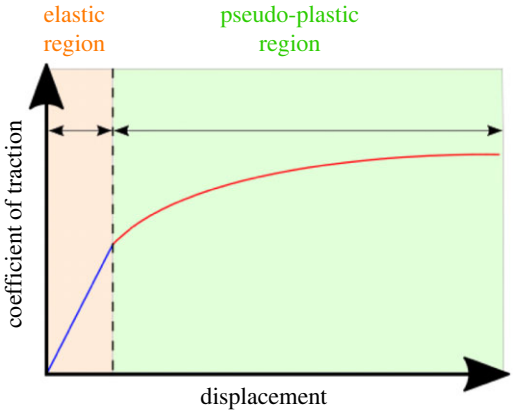

Figure 3. Example output for a HPT test [35].

crosshead (9) could be moved vertically to accommodate the test apparatus. The actuators were pressurized via a hydraulic ring main (10).

An example output for an HPT test conducted with no contaminants has been included in figure 3. The output is plotted as the rotational displacement versus the ratio of shear to normal stress, i.e. the coefficient of traction (CoT). The initial steep linear increase is labelled as the 'elastic' region (ER), followed by a flattening of the curve labelled the 'pseudo-plastic' region (PPR).

Before the application of any contaminant, the specimens were run-in using dry conditions and thereby creating a steady CoT between runs (especially important in clean contact conditions).

Tests were conducted at a pressure of 900 MPa and ambient (room) temperature, with no additional heating or cooling.

To create the leaf layer, 25 mg of leaf powder was applied in conjunction with 20 µl of distilled water. A conditioning run was then undertaken followed by a second application of 20 µl of distilled water. After this, the leaf layer was considered fully formed and measurement runs began. The formation process of the leaf layer is included in figure 4.

(iii) Analysis techniques for assessment of composition of leaves and films

Although much is known about the make-up of plant cell walls, as shown in figure 5, far less is understood about what happens to them when put in the extreme contact of the wheel/rail interface (of greatly increased pressures and temperature) relative to their usual, terrestrial environment.

Leaves are mostly composed of polysaccharides (such as pectins and other biopolymers like cellulose) and phenolic (phenol, the aromatic alcohol, being the prototypical example of these classes) compounds.

Leaves. Leaf components have differential extractability in solvents, allowing for their fractionation and following analysis. Determinations were carried out on small aliquots (mg) in triplicate. Results are referred as a proportion of the dry weight.

Analysis of the polysaccharides fraction. **Pectins:** Pectins were extracted from 10 mg samples with water at 120°C for 1 h, centrifuged and the liquid fraction (supernatant) recovered (esterified pectins). The remaining solids were treated with CDTA (*trans*-cyclohexylene-1,2-diamine-*N*,*N*,*N*′,*N*′-tetraacetate, 50 mM) overnight at room temperature to disrupt Ca^{+2} and other divalent cations bonds. The resulting supernatant fraction (non-esterified pectins) was pooled with the esterified pectins to obtain the total pectins fraction. The monosaccharide content of this fraction was determined following hydrolysis with trifluoroacetic acid (TFA, 4 h at 100°C) to break the polysaccharides into their constituent monosaccharides. Samples were dried in a vacuum centrifuge to evaporate the TFA, washed with isopropanol and resuspended

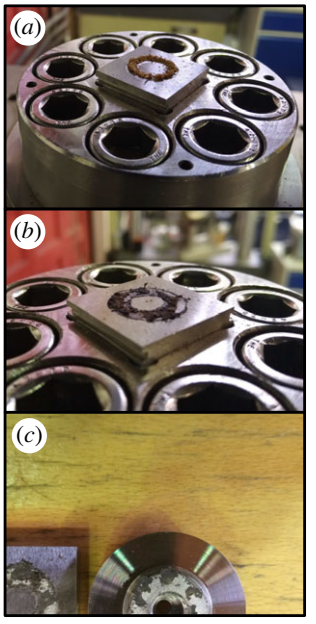

Figure 4. Leaf layer formation in the HPT test rig: (*a*) leaf powder; (*b*) after initial run-in; (*c*) after three test runs. For scale, the sizes of the samples pictured are: 30 mm (square specimen), with the top specimen having an outer diameter of 18 mm and an inner diameter of 10.5 mm.

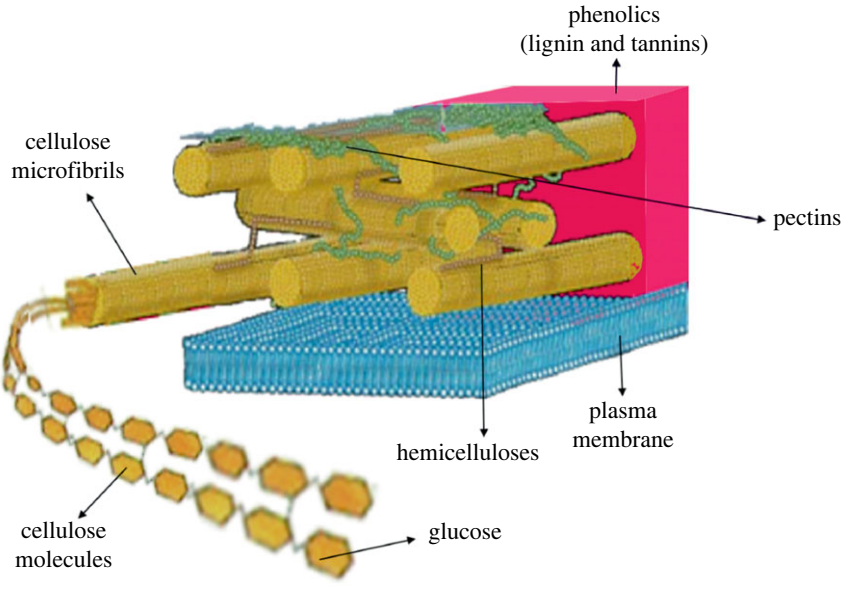

Figure 5. Schematic of a plant cell wall, detailing the key components.

in water. Identification of the major polysaccharides present was carried out through high-performance anion-exchange chromatography (HPAEC, Dionex—ThermoFisher) equipped with Pulse Amperometric Detection [36].

Hemicelluloses: The hemicellulose fraction from the matrix polysaccharides was obtained after TFA hydrolysis of powdered leaf samples (4 mg) as described above, and the major polysaccharides present in the hydrolysate were determined and quantified through HPAEC.

Cellulose: To determine the cellulose content (crystalline fraction), the remaining solids were treated by sequential hydrolysis with a 72% w/v sulfuric acid solution for 4 h at room temperature, followed by hydrolysis with a diluted (3.2%) sulfuric acid solution at 120°C for 4 h. The resulting free glucose content was determined using Anthrone [37].

Polyphenols fraction analysis. Soluble phenolics were extracted by incubating powdered leaf samples (10 mg) with 95% methanol for 48 h at room temperature, and the total phenolics content of the supernatant fraction was determined through a modified version of the Folin–Ciocalteau colorimetric method [38].

The total phenolic content was determined using the acetyl bromide method [39]. This method consists of two steps: the first one breaks down the polymeric phenolic structures and the second one conjugates the resulting structures with a chromophore that absorbs UV light. In brief, samples were incubated in an acidic solution of acetyl bromide (25% acetyl bromide in acetic acid) for 3 h at 50°C to solubilize phenolics and lignins. Following the addition of NaOH and hydroxylamine, samples were diluted with acetic acid and the absorbance was read at 280°nm. The percentage of acetyl bromide soluble phenolics/lignin (%ABSL) was determined using the formula described by Foster *et al*. [39] with an appropriate coefficient (Poplar = 18.21).

Pyr-GC–MS analysis. To obtain a more detailed compositional profile of leaves, intermediate film (IMF) and fully formed film (FFF), samples were further analysed using pyrolysis-gas chromatography–mass spectrometry (Pyr-GC–MS). Pyr-GC–MS involves the conversion to gas phase of the sample in the absence of O_2 and the resulting products are separated by gas chromatography and mass spectrometry. Samples were analysed using a 'CDS 5250-T Trapping Pyrolysis Autosampler', Agilent Technologies 7890B GC System and Agilent Technologies 5977A MSD as mass spectrum unit. The samples were pyrolyzed at 450°C for 15 s, under trapping mode. The volatile materials released were carried into the GC/MS unit, via a heated transfer line (340°C) in an He flow for GC/MS analysis. The following GC/MS parameters were applied: GC inlet temperature at 350°C, the initial temperature at 40°C for 2 min, ramp rate at 10°C/min until 300°C, holding at 300°C for 12 min, split ratio 50 : 1. Helium carrier gas flow was 1 ml min^{-1} and the separation was performed using an Agilent HP-5ms Ultra Inert (30 m × 0.25 mm × 0.25 µm) column. Volatile compounds were identified by comparing the mass spectra with the National Institute of Standards and Technology (NIST) 14 library database (Match ≥ 85%).

Inductively coupled plasma-mass spectrometry (ICP-MS) analysis. To determine whether metal contents changes during film formation, leaves, IMF and FFF were analysed through (ICP-MS). This method identifies and quantifies metal components in materials after complete acid hydrolysis of organic components. Three replicates were prepared for oak and sycamore. Fifty milligrams of sample was weighed into a digestion vessel and 8ml of concentrated HNO_3 and 2 ml of 30% H_2O_2 were added. The digestion vessels were sealed and placed into a microwave (Milestone Ethos Up). A thermocouple was placed into the digestion vessel to monitor the temperature. The microwave was programmed to heat the contents of the digestion vessels to 200°C for 30 min. Once at the desired temperature, contents were held at 200°C for 15 min. After this, the digestion vessels were cooled down before diluting to 100 ml with distilled water. 10ml of each sample was used for subsequent analysis. An environmental stock calibration fluid (ICP-MS calibration, Agilent part number 5183-4688), with a known concentration of many common elements found in the environment, was used to produce low (Ag, Al, As, Ba, Be, Cd, Co, Cr, Cu, Mn, Mo, Ni, Pb, Sb, Se, Th, Tl, U, V, Zn: 10 000 ppb) and high (Ca, Fe, K, Mg, Na: 1 000 000 ppb) concentration calibration standards. Samples and calibration solutions were run on an Agilent 7700× ICP-MS equipped with a helium collision cell.

XPS. Railhead scrapings were also obtained from UK rail network sites (Wiltshire and Yorkshire) to allow for comparison with leaf layers created at QRTC. These scrapings were then pressed into indium foil (an element not associated with plants or railway infrastructure) which was mounted on a paper label on the XPS sample holder. The interleaved paper label was used

to ensure that the scraping and indium foil were insulated from the sample holder to reduce the chance of differential charging should some parts of the scraping sample be conductive while other parts are insulating. The analyses were carried out using a Kratos Supra instrument with a monochromated aluminium source, and two analysis points per sample, of area 700 µm by 300 µm. Survey scans were collected between 1200 and 0 eV binding energy, at 160 eV pass energy, 1 eV intervals and 300 s/sweep with two sweeps being collected. High-resolution O 1s, C 1s, N 1s, Si 2p, Fe 2p and Fe 3p at 20 eV pass energy and 0.1 eV intervals for each analysis point over an appropriate energy range, with one 300 s sweep for all spectra, except the N 1s and Fe 2p regions for which two sweeps were collected. Charge neutralization of 0.25 A was used throughout. The data collected was calibrated in intensity using a transmission function characteristic of the instrument to make the values instrument independent.

The data were quantified using theoretical Schofield relative sensitivity factors modified to account for instrument geometry, variation in penetration depth with energy and the angular distribution of the photoelectrons. The high-resolution spectra were calibrated in eV by fixing the main C 1s peak to be 285.0 eV.

FT-IR. FT-IR analyses in this study were performed using a Perkin Elmer Frontier (CNAP, University of York, UK). Spectra were collected in the absorption band range of 800– 2000 cm^{-1} under room temperature. A total of 32 scans were averaged for each sample at 4 cm^{-1} resolution. Before principal component analysis (PCA), the data acquired was exported to 'R' to generate '.C files'. This process produced a matrix of peaks, unique for PCA analysis. Three spectra were collected for each sample, and the triplicate-averaged spectrum was used for PCA. The raw data were normalized and then baseline it using linear baseline correction. PCA was carried out using 'The Unscrambler *X*' 10.5.1 software (CAMO).

3. Results

A broad dataset combining tribological and biochemical information has been compiled to help establish the mechanisms and reactions occurring within the wheel/rail contact. Traction data from the HPT testing is presented with and without contaminants and in addition, biochemical analyses were carried out on selected samples to gain further insights into the composition of the materials. XPS data from leaf films taken from main line UK rail is also presented to complement the analysis.

(a) Coefficient of traction data

Tribological experiments were carried out on the HPT to assess the effect of different leaves and other low adhesion contaminants on coefficients of traction in the contact. The results from the tests of leaves (oak and sycamore), oak bark, water and a representative sample of 'clean rail' (steel) are presented in figure 6.

There is a large difference in the CoT between the clean rail (metal-on-metal) contact with a CoT above 0.7 when compared to the samples with contaminants/biomaterials in the contact (CoT ranges within 0.025–0.06). Wet rail data are included to demonstrate the effect of water in the contact. Additional comments on the mechanism of this are explored in the discussion. Figure 7 shows results from all of the tests (n.b. the scale change in the *Y*-axis) between different materials.

The CoT data show that leaves and other contaminants (graphite, oak bark powder) tested are broadly within the same CoT range, with the maximum difference being only 0.035. For reference, a CoT value of 0.05 and below would be regarded as 'ultra-low friction' within rail tribology [2]. At this point and below both braking and acceleration are greatly inhibited [2]. These results can be compared with other testing methods such as the 'HAROLD' full-scale wheel/rail test rig, which also found ultra-low friction values when testing with leaves in the contact [40].

Oak Bark powder gives slightly higher CoT values than the rest of the samples, while graphite, used as the 'low friction control', gives the lowest values.

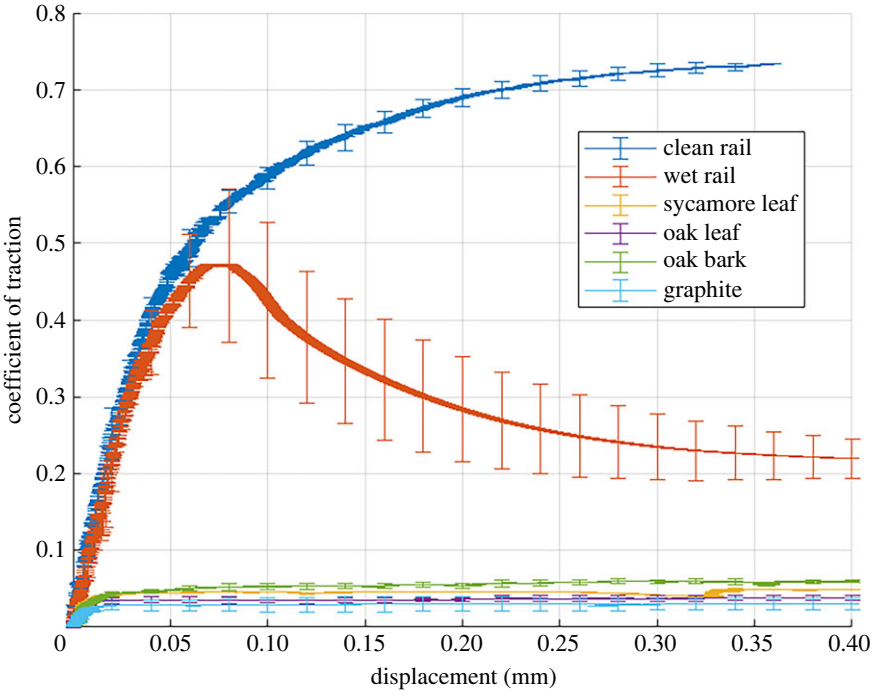

Figure 6. HPT data of all samples including a clean rail and graphite reference. Reference data for 'wet' and 'clean' rail sourced from co-authors' previous publication [34].

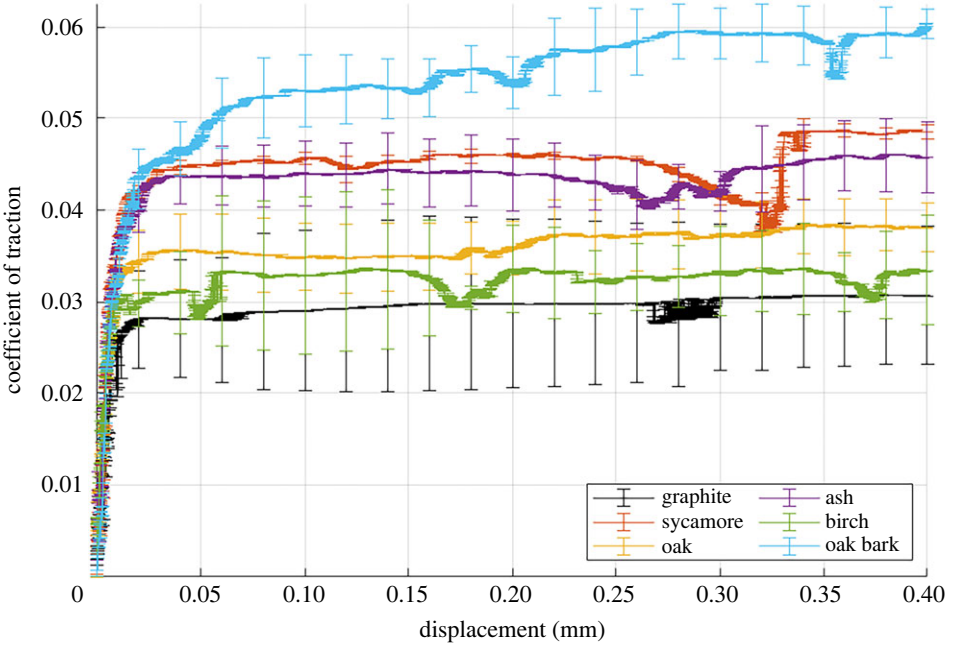

Figure 7. HPT data of different rail contaminants. Only oak and sycamore were taken for detailed analysis after this point.

Table 2. %Atomic concentration data from XPS analysis of two locations.

location/ %atomic concentration	Fe2p	O1s	N1s	Ca2p	C1s	P2s	Si2s
Wiltshire	1.3	23.7	1.1	0.6	71.8	0.2	1.3
Yorkshire	0.2	22.1	0.7	0.6	75.8	n.d.	0.5

Table 3. Compositional analysis of the polysaccharide fractions (cellulose, hemicelluloses, pectins) and phenolics fractions (total phenolics, tannins) of oak and sycamore fallen leaves and railhead films. Values represent % of dry mass (mean ± standard deviation of three replicates). IMF, intermediate film; FFF, fully formed film.

species	sample type	cellulose	hemicelluloses	pectins	total phenolics	tannins
oak	leaves	11.15 ± 0.5	17.01 ± 1.3	6.25 ± 1.99	24.43 ± 1.13	4.26 ± 0.09
	IMF	7.51 ± 1.16	8.74 ± 0.19	5.98 ± 1.25	45.87 ± 0.57	3.01 ± 0.13
	FFF	6.74 ± 2.51	8.34 ± 0.85	5.59 ± 1.44	51.51 ± 3.5	1.07 ± 0.17
sycamore	leaves	9.41 ± 0.19	12.91 ± 0.82	6.20 ± 6.47	20.11 ± 0.98	5.31 ± 0.28
	IMF	6.71 ± 1.1	9.00 ± 0.25	6.13 ± 1.57	43.08 ± 3.22	3.69 ± 0.24
	FFF	6.80 ± 1.74	9.84 ± 0.23	7.07 ± 1.57	44.14 ± 3.9	3.05 ± 0.13

(b) XPS data from railhead leaf contamination

XPS analysis gathers information on the surface of materials and scans only the top 5–10 nms of the sample [41]. XPS detects all elements to varying sensitivities, except for the lightest such as hydrogen, helium and lithium. Of those, only hydrogen is relevant to this study and can be assessed in other ways. These data are presented in table 2.

Large amounts of both carbon and oxygen are present in the samples as detected by XPS. This is in addition to inorganic elements associated with rail infrastructure (Fe), sanding treatments (Si and O) and trace minerals. The proportion of C and O suggest that the sample is largely composed of organic structures.

(c) Compositional analysis of leaves and rail films

After testing, samples were analysed using a variety of techniques to establish their composition and the chemical modifications during the formation of the films. These analyses were conducted on (i) leaf powder, (ii) IMF formed by passing a diesel shunter over leaf powder without braking for a minimum of five times and (iii) FFF produced by braking on IMF. Compositional analysis (table 3) of the main fractions that constitute fallen leaves biomass and railhead films show a decrease in the main polysaccharides fractions (cellulose, hemicelluloses) in films compared to leaves, with little change observed in the pectins. By contrast, the total phenolics fraction increases drastically in films compared to leaves, while the soluble phenolics fraction (tannins) decreases, suggesting a loss and/or insolubilization of phenolics during film formation.

Similar compositional changes were also observed in data collected from FT-IR analysis (figure 8). FT-IR profiles show that most of the regions affected correspond to wavelengths associated with polysaccharides (cellulose and hemicellulose, both non-aromatic species) and phenolic (aromatic alcohols, –OH groups) components in both species (figure 8*a*,*b*). Aromatic, or carbon–carbon double bonds, appear at different wavelengths to non-aromatic (carbon–carbon single bonds) species. This helps differentiate cellulose and its derivatives from phenolics.

The peak numbers shown in the figure correspond to: 1—1740–1735 cm^{-1}: C=O. Acetyl and methyl esters, PGA. Pectins; 2—1608–1550 cm^{-1}: COO–, PGA. Pectins; 3—1513 cm^{-1}: Guaiacyl ring, lignin/tannins; 4—1460 cm^{-1}: C–O stretching in ester and amide; 5—1441 cm^{-1}: CH, CH2; PGA. Pectins; 6—1361 cm^{-1}: CH in plane deformation, cellulose; 7—1315 cm^{-1}: OH, CH2, CH.

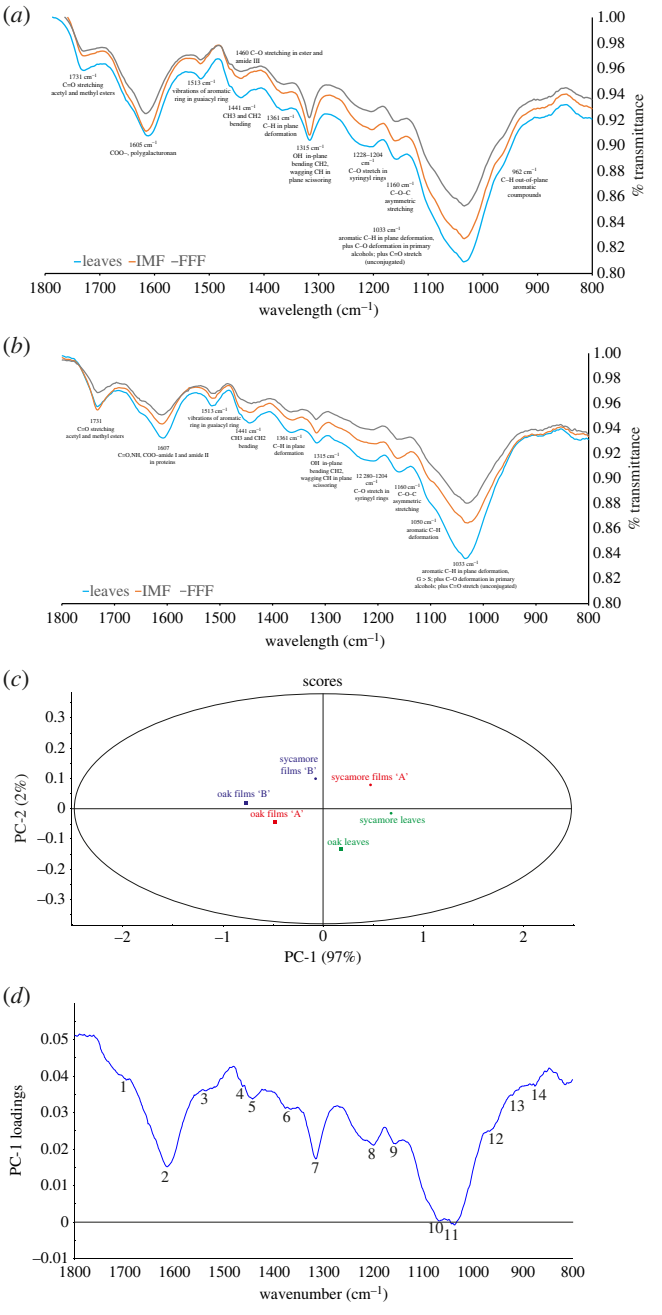

Figure 8. FT-IR analysis of oak and sycamore leaf samples and their corresponding intermediate (IMF) and fully formed (FFF) films. (*a*,*b*) FT-IR profiles of oak (*a*) and sycamore (*b*) samples. The black lines correspond to leaves, orange to IMF and blue to FFF. (*c*) Principal component analysis scores for leaves and films from both species. (*d*) Loadings analysis of principal component 1 (PC-1) showing the high impact of polysaccharides (cellulose, hemicellulose, pectins) and lignin/tannins compounds between different samples. *FT-IR assignments from 'D'*: 1—1740–1735 cm^{-1}: C=O. Acetyl and methyl esters, PGA. Pectins. 2—1608–1550 cm^{-1}: COO–, PGA. Pectins. 3—1513 cm^{-1}: Guaiacyl ring. Lignin/tannins. 4—1460 cm^{-1}: C–O stretching in ester and amide. 5—1441 cm^{-1}: CH, CH2; PGA. Pectins. 6—1361 cm^{-1}: CH in plane deformation. Cellulose. 7—1315 cm^{-1}: OH, CH2, CH. Cellulose. 8—1228–1204 cm^{-1}: C–O stretch in syringyl rings. Lignin/tannins. 9—1160 cm^{-1}: C–O–C asymmetric stretching. Cellulose. 10—1050 cm^{-1}: Aromatic C–H deformation. Lignin/tannins. 11—1033 cm^{-1}: Aromatic C–O, C=O. Lignin/tannins. 12—962 cm^{-1}: CH aromatic compounds. Lignin/tannins. 13—898 cm^{-1}: C–O–C stretching. Cellulose. 14—875 cm^{-1}: glycosidic linkage. Hemicellulose.

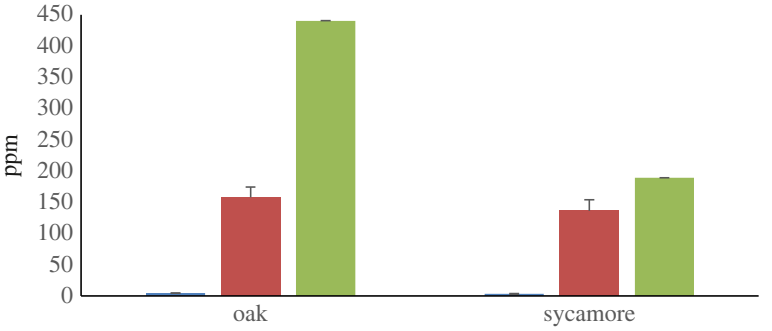

Figure 9. Content of Fe in oak and sycamore leaves (shown in blue), intermediate films (IMF, red) and fully formed films (FFF, green). Values represent the mean ± standard deviation of three replicates. ppm, parts per million.

Cellulose; 8—1228–1204 cm^{-1}: C–O stretch in syringyl rings, lignin/tannins; 9—1160 cm^{-1}: C–O–C asymmetric stretching, cellulose; 10—1050 cm^{-1}: aromatic C–H deformation, lignin/tannins; 11—1033 cm^{-1}: aromatic (phenolic) C–O, C=O, lignin/tannins; 12—962 cm^{-1}: CH aromatic (phenolic) compounds, lignin/tannins; 13—898 cm^{-1}: C–O–C stretching, cellulose; 14—875 cm^{-1}: glycosidic linkage, hemicellulose. Literature precedents for the assigned peaks are available [42].

Principal component analysis (PCA) of the FT-IR data indicates that the variation in the data is strongly explained (97%) by one component, while a second component explains 2% of the variability (figure 8*c*). The analysis of the loading in the variability (figure 8*d*) between leaves and films can be accounted for by the differences in components related to phenolics (lignin and tannins) and polysaccharides (cellulose and hemicellulose derivatives).

There is evidence from previous work indicating the participation of phenolics and iron in railhead film formation [5]. ICP-MS analysis showed a considerable increase in iron (Fe) content in films compared to IMF and fallen leaves in both species (figure 9), supporting this hypothesis. Notably, besides a modest increase in copper (Cu) content, the content of the other metals determined remained unchanged during film formation (data not shown). A variety of other elements were detected but in far lower quantities than iron.

Although Fe is an essential plant component involved as a cofactor in a number of metabolic processes, it is considered as a micronutrient as it is present in low amounts in most plant tissues. Interestingly, while metabolically active tissues have a median Fe content of 250 ppm, metabolically inactive tissues have very low amounts of iron, with wood containing no iron at all [43]. Leaves suffer a process of nutrient removal through 'senescence' and by the time that abscission happens they are expected to have very low amounts of Fe left, such as the values found in our analysis of the two leaf species (3–4.5 ppm). The opposite trend is seen in both stages of the film formation.

4. Discussion

Our results show novel evidence regarding the effect of leaf derived films on the wheel/rail friction, as well as the chemical transformations that occur in the process of film formation. We have found that both leaf powders and oak bark gave very similar CoT values to that of graphite. This effect is not from the addition of water in the system, as a much higher and different CoT curve is produced in this case.

This would suggest that the low adhesion observed is not only due to water soluble components of leaves, but also to other materials. Therefore, we conducted a complete compositional analysis to understand the materials involved in the formation of the low adhesion films.

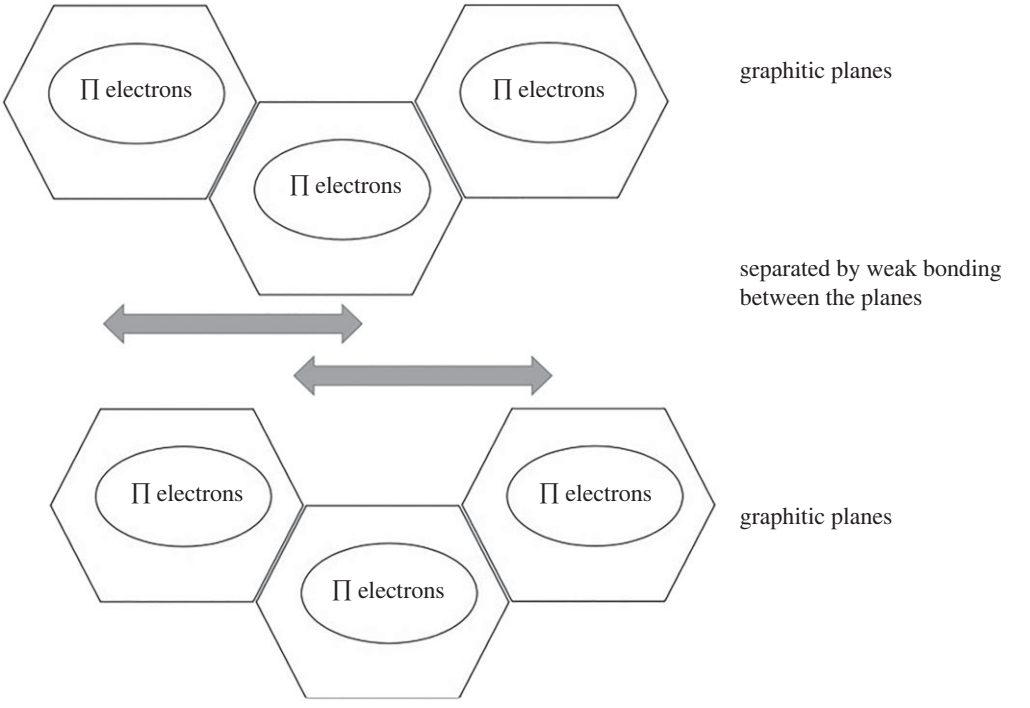

Figure 10. Schematic of 'easy-shear' lubrication, innately present in graphite and graphitic compounds due to strong bonds within the plane, and weaker forces between the two graphitic planes.

(a) Wet rail

Traction values for wet rails were included to aid the understanding of the various components influencing the system. Leaf litter encountered around railway infrastructure will have a residual moisture content. As such, the role of water needs to be considered in this context. In specific circumstances, low amounts of water can generate ultra-low friction values in the contact [2].

Metal oxides in combination with water have an interesting effect in the contact. The amount of water and iron oxide, as well as the sample's surface roughness influence the adhesion conditions. Previous work has established that a reduction of adhesion occurs due to the presence of iron oxides and trace amounts of water in the contact. However, this reduction of adhesion is limited to a narrow range of conditions [44]. XPS data showed that Fe is present in varying concentrations depending on sample geographical location (and frequency of route traffic) predominantly as Fe(III). The authors note several iron oxides and 'iron oxide-hydroxides' could play a role in the systems behaviour as have been highlighted in other works [45,46].

The authors explain that a third body layer is able to form and evolves during testing, as water evaporates. The mixture influencing friction is comprised of water, metal oxides and wear debris. This oxide–water mixture is fully removed with successive passes, as the water evaporates [44].

The 'wet rail' data presented in figure 6 show this evolution with initially higher CoT values that reduces to a steadier state as the water evaporates, leaving behind metal oxides in the interface. It is noted that although water does reduce friction, it does not do so to the same extent as the biomass tested (or indeed the graphite control data).

(b) Graphite

As expected, graphite reduced CoT values when applied to the contact surface. Graphite acts as solid lubricant due to its structural configuration (figure 10). Strong bonding is present in

the horizontal plane, with only weak (Van der Vaal's) forces being present between graphitic layers. This facilitates 'easy-shear' behaviour [47]. Graphite has been used extensively as a lubricant highlighting its capacity to wear resistance between surfaces. This is partially due to the delocalized electrons associated with graphite, coupled with 'aromatic stabilization' (where specific carbon compounds are arranged in energetically favourable conformations that resist change) [48,49].

Graphite is a well-known solid lubricant that is composed of long planar sheets of 6-ring carbons with delocalized electrons [50]. These sheets arrange themselves in order to lower the energy between the sheets. This is achieved by the strong planar bonds (through the carbon–carbon bonding) in one plane with much weaker inter-planar bonding. The weaker bonding is attributed to less strong intramolecular bonds like Van Der Vaal's forces [51]. The CoT values for the leaf derived layers are similar to those of graphite. This suggests a similar mechanism of easy-shear lubricity influencing the low adhesion behaviour seen with leaf derived layers. Furthermore, the aromatic stability associated with graphite and benzene/phenols exemplifies which types of materials are able to withstand the harsh conditions associated with the wheel/rail interface.

Leaves and biomaterials are very different in structure to the common forms of carbon. Graphite is almost completely composed of sp^2 hybridized carbon atoms. Biomaterials are composed of a number of elements (C, H, N, O, P, S and various metals), as well as having functional groups (including alcohols and organic acids) and different spatial conformations. However, when tested on the HPT, leaf samples give only slightly higher CoTs than graphite (with oak bark again being higher than leaves) as shown in figure 7. With previously tested contaminants, such as water, in the contact the CoTs obtained were significantly higher. This indicates that water alone (or water + soluble leaf extracts) does not exert the same degree of friction reduction as found in graphite of leaf powder.

Tribological contacts are very challenging to lubricate due to the high pressures (800 MPa and above for this application) and temperature spikes that can occur at metal-on-metal contacts. Graphite is known to be thermally stable and has the intrinsic ability to dissipate friction forces [52,53]. Solid lubricants like graphite are suitable for applications at extremely high temperatures and under high loads [54].

(c) Process of film formation from leaves

The changes in composition in the formation of the film from leaf powder indicates the type of changes occurring under the conditions present in the wheel/rail contact area. More importantly, our results show that the low adhesion film is composed of a network of polysaccharides and phenolic structures that incorporate Fe from the railhead. The compositional changes show the loss of hemicellulosic material during the formation of the film, and to a lesser extent the loss of cellulose. The monosaccharide profile of the hemicellulosic fraction shows a general, non-specific reduction in the neutral monosaccharides. These results are in agreement with the increase in peaks from sugar derived compounds observed in the Pyr-GC–MS analysis. The pectin content, on the other hand, remains relatively constant (or increases slightly) during film formation, suggesting that these polymers may play a role in the final film structure.

The loss of hemicellulose and cellulose in films is concomitant with an increase in the insoluble phenolic fraction. The soluble phenolics (tannins) are reduced in most species, indicating either loss of these compounds or insolubilization, likely due to the temperature and pressure produced during the film formation.

The largest oxygen component observed is at a binding energy, 533.1 eV, typical for oxygen within cellulose [55]. Organic C–O and metal hydroxide species were detected at 531.8 eV (Wiltshire) and 531.3 eV (Yorkshire).

The leaf powders tested exhibit lower CoT traces than wet rail alone. Previous studies by Cann [56] established that leaf extracts tested on a mini traction machine do cause a drop in adhesion.

In addition to pectin, both cellulose and hemicellulose are main components of the polysaccharides fraction. The effect of both iron and copper ions on the degradation of cellulose is mediated by oxidative reactions catalysed by these transition metals in the presence of O [57]. The potential for oxidation at the wheel/rail interface is high due to ambient oxygen in the air combined with the tribocontact conditions. Our results show not only a decrease in the cellulose fraction, but also an increase in cellulose derived compounds such as furans in the films.

'Iron gall ink' (made from iron salts and tannic acids) has previously been shown to cause: 'Degradation of cellulose in historic paper by iron gall ink is a synergistic process of both, acid hydrolysis caused by acidic ink ingredients and oxidation, catalysed by free iron and/or copper ions' [58–60]. This is clearly of relevance in this application which has all the components necessary for cellulose degradation; an abundance of reactive iron (and some copper) as well as oxygen and heat.

Lignin (a key component in woody materials) can also be modified in the presence of iron compounds such as a 'Lewis acid' (iron trichloride) that produces partial hydrolysis of the phenolic structures [27].

(d) Potential catalytic routes for the conversion of leaves to 'black layer'

The conversion of leaf powder within representative wheel/rail contact conditions indicates catalytic activity of some nature. As shown in table 2, leaf powder initially has a high cellulose content and a relatively lower polyphenol content.

The polyphenol content increases in a stepwise manner, while the cellulose fraction decreases (IMF versus FFF).

Iron based catalysts have been explored for their ability to convert biomass components into different structures. One example is the hydro-deoxygenation of lignin vapours using Fe catalysts [61]. Products from this were found to be benzene, toluene, xylenes, phenol, cresols and alkyl phenols, all of which have aromatic components, imparting 'aromatic stability' onto the breakdown products. This property is associated with the cyclic delocalization of electrons, resulting in extra stabilization of aromatic species [62]. This type of stabilization could be involved in the strongly bonded layer derived from leaf degradation.

There are many examples in the literature of iron or iron derived species being able to break down large biopolymers. Under mild acidic conditions, Fe polyphenolate conversion films can form on iron surfaces by precipitation of Fe(III) cations with polyphenolic molecules containing a free catechol group. These groups are 'bidentate' ligands able to complex iron. This polyphenolic, organic structure affects the morphological properties of the conversion film [63]. Perhaps of most relevance is the use of a solid iron salt catalyst for selective conversion of biomass-derived sugars [8].

These observations, taken together with our data, suggest that biomass on the railhead would undergo oxidative reactions in the presence of iron (from the railhead), within the contact patch.

(e) Mechanisms of lubrication

The wheel/rail interface is a challenging environment as not only is it under high pressure but also high temperatures. The literature suggests that as long as the creep value is lower than 2% and the 'coefficient of friction' (faithfully reproduced [sic]) is below 0.6, the temperature should not exceed 450–500°C, based on numerical modelling [64].

Studies on the effects of iron as an oxidative catalyst on biomass show that cellulose can be oxidized in the presence of rusting iron to form 'oxycellulose' compounds, as well as depolymerize xylans and glucans [65]. Fenton reactions are the most likely route for these changes.

Previous studies confirmed that cellulosic materials in tribocontact produce a combination of cellulose and carbon fibres that show lower strengths, even at low contact pressures [66]. It has also previously been reported that biomass components such as lignin can affect friction values,

especially when exposed to heat. In agreement with our observations, chemically treated walnut shells increased in lignin content, and thus could be used as an effective lubricant, suppressing the fade phenomenon of the final composite during friction test at elevated temperatures [67].

Our data show that under high pressure and elevated temperature conditions (representative of the wheel/rail interface) biomass components partially degrade and the composition of the final film is enriched in insoluble phenolics. The increase in polyphenols indicates that these species re-arrange under the harsh conditions associated with the wheel/rail contact. Polyphenols share some chemical similarities with graphite in that they have a large portion of pi-electrons (associated with aromatic compounds) and are structurally much more confined (although not completely planar, like graphite). This is supported by our data on the coefficients of traction of these materials. Hentschel established that traction coefficients are strongly dependent on the chemical structure of the lubricants (in this case, leaf matter) [28]. Hentschel also noted high coefficient values mostly arise from lubricants whose molecules are arranged in structures that allow only heavily hampered rotational intramolecular motions along single bond axes. Low coefficients were derived from molecules that have thread-like interactions and a minimum of structural subunits or functional groups which are involved in intermolecular interactions [28].

Previous tribological research has established that the lubrication behaviour of 'polynuclear aromatics' (more commonly known as poly-cyclic aromatic hydrocarbons, PAHs) is determined by the ease with which they can form a stable radical anion [68]. PAHs alone exhibit 'low friction' with a 'highly polished' surface observed, producing an 'insoluble' crystalline product—all of which are characteristic of the 'black layer' found on railheads.

Our work establishes that the leaf components undergo chemical transformations at the wheel/rail interface, forming tenacious thin film that is hard to remove either chemically (citra-solv) or mechanically (wire brush scrubbing). Tannins and polyphenols are aromatic structures and are well known for their stability and resistance to oxidation. Aromatic species have already been explored within automotive tribology [69] where the mechanism of lubricity resides in their structural characteristics. Aromatic compounds lubricity is due to repulsion of π-electrons (C=C bonded carbons) and these have little unevenness (planar structure) for interlocking [69]. Besides, tannins have the capacity to bind to iron, as present in the railhead [70]. Previous researchers have found that benzene produces a lower CoT than other cyclic compounds due to π-electrons above and below the molecular plane, inducing repulsion of the negative charges when two molecules become close. Literature data showing 'aromatic' species like benzene and chloro-benzene give far lower CoTs than non-aromatics such as bi-cyclo-hexyl/bicyclohexane species [28].

The authors conclude similar findings, that compounds containing non-aromatic carbon rings can exhibit worse lubricity, especially when compared to carbon rings that are 'aromatic' (such as benzene and phenol).

Our data show the changes observed within leaf material at the wheel rail/contact into a semi-stable, thin film and shares some similarities with other proportionally high-sp^2 content planar, stable carbonaceous species. It appears highly likely that iron ions play a key role in this, by stabilizing phenolic structures and potentially by acting as a Lewis acid catalyst. An approximation of the proposed aromatically stabilized iron chelate species is given in figure 11. This type of interlayer motif when expanded to scale is seen in the well-known friction modifier Molybdenum disulfide (MoS_2), where Molybdenum atoms are sandwiched between sulfides, enabling easy-shear lubricity.

5. Conclusion

Low friction leaf derived layers were created in the laboratory and in the field to give broad insight into the mechanism of reduced friction at the wheel/rail interface. The data could suggest that biomass at the wheel/rail interface may undergo a conversion to a more stable form of planar, aromatic carbon species (such as phenolics). This potential conversion could explain how the multiple components of leaves are able to form a tenacious thin film in the contact. The formation

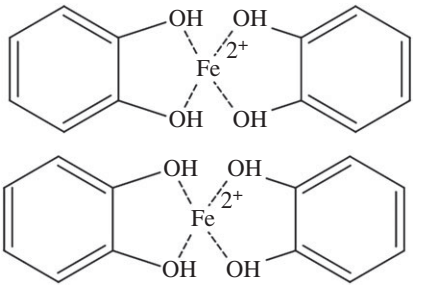

Figure 11. Simplified example of potential phenolic type chelated iron.

of a large amount of phenolic species in the contact is likely catalysed by iron ions, given the heat and pressure associated with the contact.

- Biomass is reported to be sensitive to the presence of *iron (Fe) which has the ability to catalytically break down* the larger molecules.
- The authors observe a *reduction in certain species* from the leaves tested (hemicellulose and cellulose), in tandem *with an increase in polyphenolic* compounds.
- When comparing leaf powder (prior to testing) with the FFF, *a large increase in the content of Fe is noted*, other alloying elements present in rail steel are not detected at such increased amounts.
- Aromatic compounds and similar compounds with delocalized electrons (like graphite) benefit from *aromatic stability*—indicating how they are able to *survive the contact*, where other molecules cannot.
- Mechanistic insight has been applied on how *leaves transform on a railhead* from their initial composition to a very different set of smaller components that have affinities for metals (specifically iron and copper).

This new insight into the composition of the leaf derived layer is expected to enable the development of novel remediation techniques. As the role of phenolics has been identified as key herein, remediation strategies targeting these molecules should be pursued. Enzymatic digestion may be one route to accomplish this. Another route forward is the selection of cleaning agents that are better able to solvate aromatic species, specifically when compared to the current standard of D-limonene, commonly known as 'Citra-solv' in industrial settings.

Data accessibility. The data are provided in electronic supplementary material [70].

Declaration of AI use. We have not used AI-assisted technologies in creating this article.

Authors' contributions. J.L.L.: formal analysis, investigation, methodology, writing—original draft, writing—review and editing; L.F.: formal analysis, investigation, methodology, writing—original draft, writing—review and editing; T.B.: investigation, methodology, writing—review and editing; W.A.S.: formal analysis, methodology, writing—original draft; M.P.S.: formal analysis, software, writing—original draft; R.L.: funding acquisition, supervision, writing—review and editing; L.D.G.: funding acquisition, supervision, writing—original draft, writing—review and editing.

All authors gave final approval for publication and agreed to be held accountable for the work performed therein.

Conflict of interest declaration. We declare we have no competing interests.

Funding. The authors of this paper would like to thank the Rail Safety and Standards Board (RSSB) for funding this research under project no. COF-G24-01, titled: 'Understanding the polysaccharide composition of crushed leaves and evaluating potential enzyme treatments'.

Acknowledgements. The authors would also like to thank the 'University of Sheffield Institutional Open Access Fund' in cases where this has been used. For the purpose of open access, the author has applied a Creative Commons Attribution (CC BY) license to any Author Accepted Manuscript version arising.

References

1. White B, Watson M, Lewis R. 2022 A year-round analysis of railway station overruns due to low adhesion conditions. *Proc. Inst. Mech. Eng. F J. Rail Rapid Transit* **237**, 458–469. (doi:10.1177/09544097221117314)
2. Buckley-Johnstone LE, Trummer G, Voltr P, Six K, Lewis R. 2020 Full-scale testing of low adhesion effects with small amounts of water in the wheel/rail interface. *Tribol. Int.* **141**, 105907. (doi:10.1016/j.triboint.2019.105907)
3. White B, Nilsson R, Olofsson U, Arnall AD, Evans MD, Armitage T, Fisk J, Fletcher DI, Lewis R. 2018 Effect of the presence of moisture at the wheel–rail interface during dew and damp conditions. *Proc. Inst. Mech. Eng. F J. Rail Rapid Transit* **232**, 979–989. (doi:10.1177/0954409717706251)
4. Jendel T. 2000 *Prediction of wheel profile wear*. Stockholm, Sweden: Institutionen för farkostteknik.
5. Pau M, Aymerich F, Ginesu F. 2002 Distribution of contact pressure in wheel–rail contact area. *Wear* **253**, 265–274. (doi:10.1016/S0043-1648(02)00112-6)
6. Mok WSL, Antal MJ. 1983 Effects of pressure on biomass pyrolysis. II. Heats of reaction of cellulose pyrolysis. *Thermochim. Acta* **68**, 165–186. (doi:10.1016/0040-6031(83)80222-6)
7. Figueiredo A, Evtuguin D, Saraiva J. 2010 Effect of high pressure treatment on structure and properties of cellulose in eucalypt pulps. *Cellulose* **17**, 1193–1202. (doi:10.1007/s10570-010-9454-2)
8. Sun K, Shao Y, Liu P, Zhang L, Gao G, Dong D, Zhang S, Hu G, Xu L, Hu X. 2021 A solid iron salt catalyst for selective conversion of biomass-derived C5 sugars to furfural. *Fuel* **300**, 120990. (doi:10.1016/j.fuel.2021.120990)
9. Xia S *et al.* 2021 Reaction kinetics, mechanism, and product analysis of the iron catalytic graphitization of cellulose. *J. Clean. Prod.* **329**, 129735. (doi:10.1016/j.jclepro.2021.129735)
10. Gallardo-Hernandez EA, Lewis R. 2008 Twin disc assessment of wheel/rail adhesion. *Wear* **265**, 1309–1316. (doi:10.1016/j.wear.2008.03.020)
11. Marshall MB, Lewis R, Dwyer-Joyce RS, Olofsson U, Björklund S. 2006 Experimental characterization of wheel-rail contact patch evolution. *J. Tribol.* **128**, 493–504. (doi:10.1115/1.2197523)
12. Suzumura J, Sone Y, Ishizaki A, Yamashita D, Nakajima Y, Ishida M. 2011 In situ X-ray analytical study on the alteration process of iron oxide layers at the railhead surface while under railway traffic. *Wear* **271**, 47–53. (doi:10.1016/j.wear.2010.10.054)
13. Zhu Y, Olofsson U, Nilsson R. 2012 A field test study of leaf contamination on railhead surfaces. *Proc. Inst. Mech. Eng. F J. Rail Rapid Transit* **228**, 71–84. (doi:10.1177/0954409712464860)
14. Poole W. 2007 Characteristics of railhead leaf contamination. Summary Report published by Rail Safety and Standards Board (May 2007). London, UK: Rail Safety Standard and Standards Board.
15. Ishizaka K, Lewis SR, Hammond D, Lewis R. 2018 Chemistry of black leaf films synthesised using rail steels and their influence on the low friction mechanism. *RSC Adv.* **8**, 32 506–32 521. (doi:10.1039/C8RA06080K)
16. Karlberg AT, Magnusson K, Nilsson U. 1992 Air oxidation of d-limonene (the citrus solvent) creates potent allergens. *Contact Dermat.* **26**, 332–340. (doi:10.1111/j.1600-0536.1992.tb00129.x)
17. John I, Muthukumar K, Arunagiri A. 2017 A review on the potential of citrus waste for D-Limonene, pectin, and bioethanol production. *Int. J. Green Energy* **14**, 599–612. (doi:10.1080/15435075.2017.1307753)
18. Cui G, Yang X, Liu Z, Wei M, Liu T, Gu H, Yang L. 2022 Potential use of limonene as an alternative solvent for extraction of Gutta-Percha from Eucommia ulmoides. *ACS Sustainable Chem. Eng.* **10**, 11 057–11 068. (doi:10.1021/acssuschemeng.2c03898)
19. Varley J. 2018 Valuing nature – a railway for people and wildlife… The Network Rail Vegetation Management Review. [pdf]. See https://www.gov.uk/government/publications/network-rail-vegetation-management-review-valuing-nature-a-railway-for-people-and-wildlife.
20. Lanigan JL, Krier P, Lewis R. 2019 Predictable and Optimised Braking: Using cryogenic technology to increase adhesion (SC04-POB-15). London, UK: RSSB.
21. Krier P, Lanigan J, Ferriday P, Lewis R. 2020 Development and implementation of novel cryogenic railhead cleaning technology. *Perm. Way Inst. J.* **138**, 35–39.

22. Lanigan J, Krier P, Johnstone LB, White B, Ferriday P, Lewis R. 2020 Field trials of a methodoglogy for locomotive brake testing to assess friction enhancement in the wheel/rail interface using a representative leaf layer. *Proc. Inst. Mech. Eng. F J. Rail Rapid Transit*. **235**, 1053–1064. (doi:10.1177/0954409720973135)
23. Watson M, White B, Lanigan J, Slatter T, Lewis R. 2020 The composition and friction-reducing properties of leaf layers. *Proc. R. Soc. A* **476**, 20200057. (doi:10.1098/rspa.2020.0057)
24. Skipper WA, Chalisey A, Lewis R. 2018 A review of railway sanding system research: adhesion restoration and leaf layer removal. *Tribol. - Mater. Surf. Interfaces* **12**, 237–251. (doi:10.1080/17515831.2018.1542791)
25. Pronti L, Perino M, Cursi M, Santarelli ML, Felici AC, Bracciale MP. 2018 Characterization and digital restauration of XIV-XV centuries written parchments by means of nondestructive techniques: three case studies. *J. Spectrosc.* **2018**, 2081548. (doi:10.1155/2018/2081548)
26. Brönsted JN, Guggenheim EA. 1927 Contribution to the theory of acid and basic catalysis. The mutarotation of glucose. *J. Am. Chem. Soc.* **49**, 2554–2584. (doi:10.1021/ja01409a031)
27. Amarasekara AS, Deng F. 2019 Single reagent treatment and degradation of switchgrass using iron(III)chloride: the effects on hemicellulose, cellulose and lignin. *Biomass Bioenergy* **131**, 105421. (doi:10.1016/j.biombioe.2019.105421)
28. Hentschel KH. 1985 The influence of molecular structure on the frictional behaviour of lubricating fluids 2: low coefficients of traction. *J. Synth. Lubr.* **2**, 239–253. (doi:10.1002/jsl.3000020205)
29. Cyrański MK. 2005 Energetic aspects of cyclic pi-electron delocalization: evaluation of the methods of estimating aromatic stabilization energies. *Chem. Rev.* **105**, 3773–3811. (doi:10.1021/cr0300845)
30. Bordwell FG, Fried HE. 1991 Heterocyclic aromatic anions with 4n+ 2. pi.-electrons. *J. Org. Chem.* **56**, 4218–4223. (doi:10.1021/jo00013a027)
31. Kuiters A, Sarink H. 1986 Leaching of phenolic compounds from leaf and needle litter of several deciduous and coniferous trees. *Soil Biol. Biochem.* **18**, 475–480. (doi:10.1016/0038-0717(86)90003-9)
32. Thompson E, Danks AE, Bourgeois L, Schnepp Z. 2015 Iron-catalyzed graphitization of biomass. *Green Chem.* **17**, 551–556. (doi:10.1039/C4GC01673D)
33. Evans M, Skipper WA, Buckley-Johnstone L, Meierhofer A, Six K, Lewis R. 2021 The development of a high pressure torsion test methodology for simulating wheel/rail contacts. *Tribol. Int.* **156**, 106842. (doi:10.1016/j.triboint.2020.106842)
34. Skipper WA, Nadimi S, Watson M, Chalisey A, Lewis R. 2023 Quantifying the effect of particle characteristics on wheel/rail adhesion & damage through high pressure torsion testing. *Tribol. Int.* **179**, 108190. (doi:10.1016/j.triboint.2022.108190)
35. Skipper W. 2021 *Sand particle entrainment and its effects on the wheel/rail interface*. Sheffield, UK: University of Sheffield.
36. Talaga P, Vialle S, Moreau M. 2002 Development of a high-performance anion-exchange chromatography with pulsed-amperometric detection based quantification assay for pneumococcal polysaccharides and conjugates. *Vaccine* **20**, 2474–2484. (doi:10.1016/S0264-410X(02)00183-4)
37. De Bruyn J, Van Keulen H, Ferguson J. 1968 Rapid method for the simultaneous determination of glucose and fructose using anthrone reagent. *J. Sci. Food Agric.* **19**, 597–601. (doi:10.1002/jsfa.2740191009)
38. Ainsworth EA, Gillespie KM. 2007 Estimation of total phenolic content and other oxidation substrates in plant tissues using Folin–Ciocalteu reagent. *Nat. Protoc.* **2**, 875–877. (doi:10.1038/nprot.2007.102)
39. Foster CE, Martin TM, Pauly M. 2010 Comprehensive compositional analysis of plant cell walls (lignocellulosic biomass) part I: lignin. *J. Vis. Exp.* **37**, e1745.
40. Lewis R, Trummer G, Six K, Stow J, Alturbeh H, Bryce B, Shackleton P, Johnstone LB. 2023 Leaves on the line: characterising leaf based low adhesion on railway rails. *Tribol. Int.* **185**, 108529. (doi:10.1016/j.triboint.2023.108529)
41. Powell CJ, Jablonski A. 2009 Surface sensitivity of X-ray photoelectron spectroscopy. *Nucl. Instrum. Methods Phys. Res. Sect. A* **601**, 54–65. (doi:10.1016/j.nima.2008.12.103)
42. López-Malvar A, Santiago R, Malvar RA, Martín D, Pereira dos Santos I, Batista de Carvalho LA, Faas L, Gómez LD, da Costa RM. 2021 FTIR screening to elucidate compositional differences in maize recombinant inbred lines with contrasting saccharification efficiency yields. *Agronomy* **11**, 1130. (doi:10.3390/agronomy11061130)

43. Ancuceanu R, Dinu M, Hovaneå£ M, Anghel A, Popescu C, Negreåÿ S. 2015 A survey of plant iron content—a semi-systematic review. *Nutrients* **7**, 10 320–10 351. (doi:10.3390/nu7125535)
44. Buckley-Johnstone LE, Trummer G, Voltr P, Meierhofer A, Six K, Fletcher DI, Lewis R. 2019 Assessing the impact of small amounts of water and iron oxides on adhesion in the wheel/rail interface using High Pressure Torsion testing. *Tribol. Int.* **135**, 55–64. (doi:10.1016/j.triboint.2019.02.024)
45. Zambrano OA, Gallardo KF, Polania DM, RodrãGuez SA, Coronado JJ. 2017 The role of the counterbody's oxide on the wear behavior of HSS and Hi-Cr. *Tribol. Lett.* **66**, 1. (doi:10.1007/s11249-017-0954-1)
46. Kempka T. 2019 *Providing predictable and optimised traction and breaking through tribo-chemical understanding of the wheel/rail interface*. Sheffield, UK: University of Sheffield.
47. Bowden FP, Young J. 1951 Friction of diamond, graphite, and carbon and the influence of surface films. *Proc. R. Soc. Lond. A* **208**, 444–455. (doi:10.1098/rspa.1951.0173)
48. Aihara J-I, Yamabe T, Hosoya H. 1994 Aromatic character of graphite and carbon nanotubes. *Synth. Met.* **64**, 309–313. (doi:10.1016/0379-6779(94)90128-7)
49. Lim Y, Park H, Caron A. 2019 Investigation on the role of interfacial water on the tribology between graphite and metals. *RSC Adv.* **9**, 7285–7291. (doi:10.1039/C8RA10584G)
50. Savage RH. 1948 Graphite lubrication. *J. Appl. Phys.* **19**, 1–10. (doi:10.1063/1.1697867)
51. Bollmann W, Spreadborough J. 1960 Action of graphite as a lubricant. *Nature* **186**, 29–30. (doi:10.1038/186029a0)
52. Wang H-D. 2013 Graphite solid lubrication materials. In *Encyclopedia of tribology* (eds QJ Wang, Y-W Chung), pp. 1550–1555. Boston, MA: Springer US.
53. Diefendorf R. 1960 *The Deposition of Pyrolytic Graphite*. Schenectady, NY: General Electric Co.
54. Carlén H. 2013 Hot applications run longer with graphite. See https://evolution.skf.com/en/hot-applications-run-longer-with-graphite/.
55. Johansson LS, Campbell JM, Rojas OJ. 2020 Cellulose as the in situ reference for organic XPS. Why? Because it works. *Surf. Interface Anal.* **52**, 1134–1138. (doi:10.1002/sia.6759)
56. Cann P. 2006 The 'leaves on the line' problem—a study of leaf residue film formation and lubricity under laboratory test conditions. *Tribol. Lett.* **24**, 151–158. (doi:10.1007/s11249-006-9152-2)
57. Kolar J. 1997 Mechanism of autoxidative degradation of cellulose. *Restaurator* **18**, 161–176. (doi:10.1515/rest.1997.18.4.163)
58. Henniges U, Reibke R, Banik G, Huhsmann E, HÃHner U, Prohaska T, Potthast A. 2008 Iron gall ink-induced corrosion of cellulose: aging, degradation and stabilization. Part 2: application on historic sample material. *Cellulose* **15**, 861–870. (doi:10.1007/s10570-008-9238-0)
59. Potthast A, Henniges U, Banik G. 2008 Iron gall ink-induced corrosion of cellulose: aging, degradation and stabilization. Part 1: model paper studies. *Cellulose* **15**, 849–859. (doi:10.1007/s10570-008-9237-1)
60. Henniges U, Banik G, Reibke R, Potthast A. 2008 *Studies into the early degradation stages of cellulose by different iron gall ink components. in macromolecular symposia*. Vienna, Austria: Wiley Online Library.
61. Olcese RN, Lardier G, Bettahar M, Ghanbaja J, Fontana S, Carré V, Aubriet F, Petitjean D, Dufour A. 2013 Aromatic chemicals by iron-catalyzed hydrotreatment of lignin pyrolysis vapor. *ChemSusChem* **6**, 1490–1499. (doi:10.1002/cssc.201300191)
62. De Proft F, Geerlings P. 2004 Relative hardness as a measure of aromaticity. *Phys. Chem. Chem. Phys.* **6**, 242–248. (doi:10.1039/B312566C)
63. Veys-Renaux D, Reguer S, Bellot-Gurlet L, Mirambet F, Rocca E. 2018 Conversion of steel by polyphenolic model molecules: corrosion inhibition mechanism by rutin, esculin, esculetol. *Corros. Sci.* **136**, 1–8. (doi:10.1016/j.corsci.2018.02.015)
64. Knothe K, Liebelt S. 1995 Determination of temperatures for sliding contact with applications for wheel-rail systems. *Wear* **189**, 91–99. (doi:10.1016/0043-1648(95)06666-7)
65. Emery JA, Schroeder HA. 1974 Iron-catalyzed oxidation of wood carbohydrates. *Wood Sci. Technol.* **8**, 123–137. (doi:10.1007/BF00351367)
66. Kowaluk G, Bartosz P, Iwona F, Remy M, Piotr B. 2010 Influence of ligno-cellulosic particles on tribological properties of boards. *Eur. J. Wood Wood Prod.* **68**, 95–98. (doi:10.1007/s00107-009-0362-9)
67. Qi S *et al.* 2014 Effects of walnut shells on friction and wear performance of eco-friendly brake friction composites. *Proc. Inst. Mech. Eng. J: J. Eng. Tribol.* **228**, 511–520. (doi:10.1177/1350650113517112)

68. Goldblatt IL. 1971 Model for lubrication behavior of polynuclear aromatics. *Ind. Eng. Chem. Prod. Res. Dev.* **10**, 270–278. (doi:10.1021/i360039a005)
69. Tsubouchi T, Hata H. 1995 Study on the fundamental molecular structures of synthetic traction fluids: part 2. *Tribol. Int.* **28**, 335–340. (doi:10.1016/0301-679X(95)00085-I)
70. Lanigan JL, Faas L, Butcher T, Skipper WA, Silva MP, Lewis R, Gomez LD. 2024 Pressure induced transformation of biomass to a highly durable, low friction film on steel. Figshare. (doi:10.6084/m9.figshare.c.7055530)